Zeitschrift für anorganische und allgemeine Chemie

Journal of Inorganic and General Chemistry
ZAAC
Zeitschrift für anorganische und allgemeine Chemie

RESEARCH ARTICLE OPEN ACCESS

Synthesis and Thermolysis of Ylidyl-Substituted Stannylenes

Pascal Weisenburger | Emily Bitzer | Christopher E. Anson | Frank Breher

Karlsruhe Institute of Technology (KIT), Institute of Inorganic Chemistry (AOC), Karlsruhe, Germany

Correspondence: Frank Breher (breher@kit.edu)

Received: 21 April 2026 | **Revised:** 13 May 2026 | **Accepted:** 18 May 2026

Keywords: density-functional theory calculations | metallacycle | phosphorus ylides | thermolysis | tin

ABSTRACT

Low-valent group 14 compounds, i.e., tetrylenes, have been subject of research since the 1970s and are still in the focus of interest. Herein, we report on the synthesis of the dimeric amido(ylidyl)stannylene $[Ph_3PCH\{SnN(SiMe_3)_2\}]_2$ (**1**) synthesized from readily available starting materials. X-ray diffraction analysis shows that the compound features a heterocyclic Sn_2C_2 core structure substituted by bis(trimethylsilyl)amido ligands. Addition of gallium trichloride led to a ligand exchange of the amide to chloride. The dimeric chlorostannylene $[Ph_3PCH\{SnCl\}]_2$ (**2**) was found to be insoluble in organic solvents but could potentially serve as a precursor to synthesize further ylidyl-substituted stannylenes with the identical structural motive. Thermal treating of **1** led to *ortho*-metalation of one Ph substituent under concomitant elimination of $HN(SiMe_3)_2$ providing the dimeric, *ortho*-metalated aryl(ylidyl)stannylene $[Ph_2PCH(\mu\text{-}C_6H_4)Sn]_2$ (**V**), which has already been described before in the literature. As a side product, we also obtained a mixture of a Sn_4C_4 heterocubane and an oligomer featuring a Sn_3C_4 core structure. Quantum chemical calculations were performed to analyze the tin–carbon interaction in the stannylenes.

1 | Introduction

The stabilization of low-valent group 14 compounds has been of general interest over the past decades [1–9]. Due to their similarity to carbenes, heavier tetrylenes have been well studied. Since the first activation of dihydrogen by a tin compound in 2008 [10], tin-based ambiphiles, including stannylenes [10], distannynes [11, 12], and Frustrated Lewis Pairs [13], have been in the focus of many groups [14].

Low-valent tin species require thermodynamic or kinetic stabilization, which can, for example, be provided by bulky amido ligands [7]. In particular, the bis(trimethylsilyl)amido ligand has been extensively used throughout the periodic table. On one hand, their steric bulk allows the isolation of low-valent compounds such as tetrylenes. On the other hand, the ligand can be used to synthesize soluble precursors [15, 16]. Ylidyl substituents are isoelectronic to amido ligands and have been applied as strong π-donor substituents with tunable donor properties [17]. Therefore, ylidyl substituents were used in the past to isolate electron-rich tetrylenes [18]. Some examples are shown in Figure 1.

The first monomeric diamido stannylene **I** was reported by Lappert and coworkers in 1974 [19]. The stannylene is nowadays used for the synthesis of starting materials [16, 20]. The first bis(ylidyl) stannylene **II** was synthesized by Schmidpeter in 1997. **II** was prepared from **I** and the bis(ylide) via deprotonation. Structurally, the stannylene is comparable to *N*-heterocyclic stannylenes by exchange of the amido group with an isolable ylidyl substituent [21]. Gessner and co-workers reported on acyclic bis(ylidyl)-stabilized tetrylenes synthesized via salt metathesis starting from metalated ylides featuring anion-stabilizing tosylate or nitril groups [22]. For the cyano-substituted ylide, the chloro-stannylene and an amido-substituted stannylene **III** were reported [23].

Dedicated to Professor Claus Feldmann on occasion of his 60th birthday.

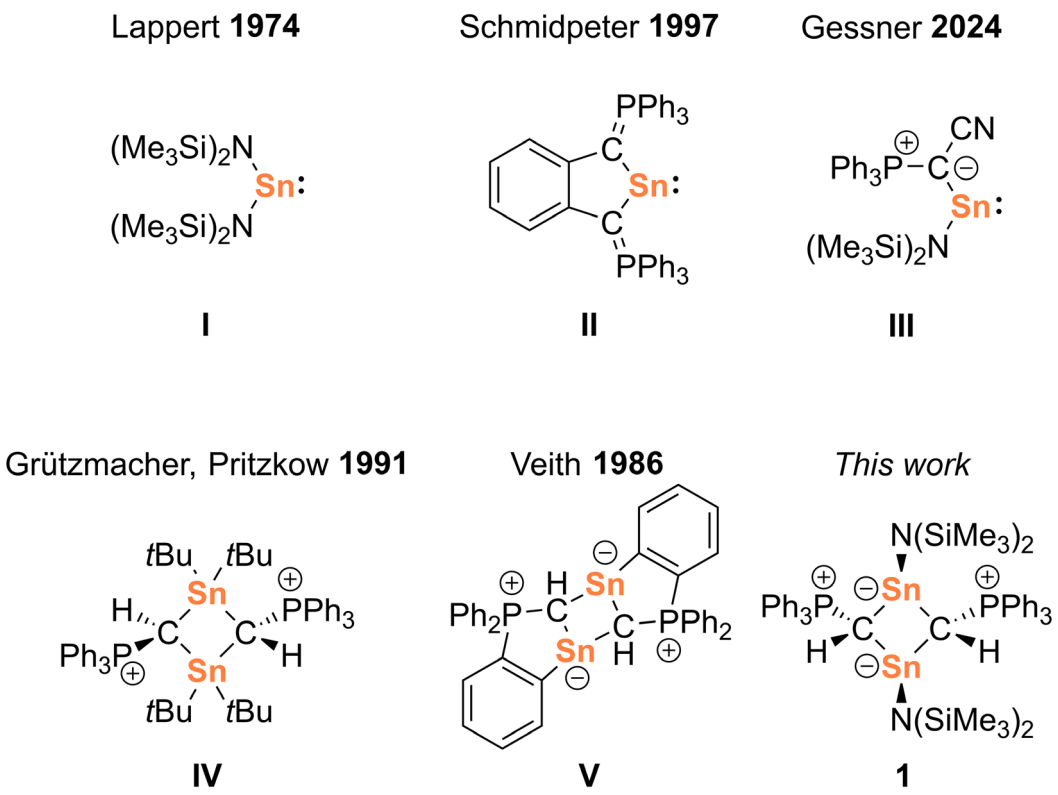

FIGURE 1 | Top: Selected examples of amido- and ylidyl-substituted stannylenes. Bottom: Dimeric, cationic group 14-substituted ylide (**IV**), *ortho*-Ylidyl-substituted stannylene (**V**), and reported stannylene herein.

Since partial double bonds can be formulated in ylidyl-substituted Main Group compounds, ylidyl-substituted stannanes and stannylenes can be seen as stannaethenes. Grützmacher and Pritzkow observed that the cationic di-*tert*-butyl substituted ylidyl stannane **IV** forms a dimer in the solid state [24]. Similar structures were obtained by our group for a cationic α-silylated ylide in 2022 [25].

Dimeric, ylidyl-substituted stannylenes were reported already in 1986 by Veith and co-workers. Synthetic access was provided through an ylide diamidostannylene adduct [26].

To further investigate the potential of ylidyl substituents derived from unstabilized ylides, we turned our attention to low-valent group 14 species.

2 | Results and Discussion

2.1 | Synthesis and Characterization

Since the reports on ylidyl-substituted stannylenes only include either cyclic compounds (e.g., **II**) or stabilized ylides (e.g., **III**), we were interested in the isolation of ylidyl-substituted stannylenes with unstabilized ylides. The diamido stannylene **I** was chosen as a soluble tin(II) precursor. When methylene triphenylphosphorane is treated with **I** in toluene, an orange solution is formed. In the ^{1}H NMR spectrum, the formation of the protonated amide, i.e., $HN(SiMe_3)_2$, can be observed. After stirring overnight, the reaction mixture was dried in vacuo and the residue extracted in hexane. From the concentrated hexane solution, compound **1** was obtained as a yellow crystalline solid in 58% yield (Scheme 1).

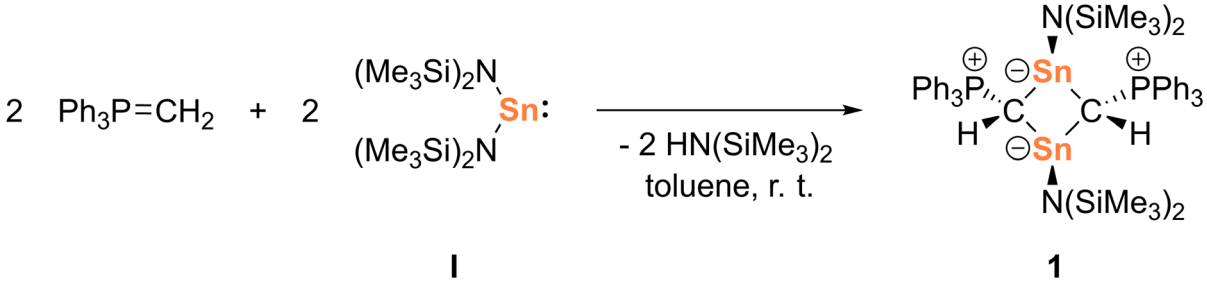

SCHEME 1 | Synthesis of **1**. Compound **1** and the following dimeric stannylenes are drawn as zwitterionic stannyl anions, but addressed to as stannylenes for better consistency with previously published ylidyl-stannylenes (e.g., **III**).

Single crystals were obtained from a concentrated solution of **1** in hexane (space group $P\bar{1}$). The molecular structure is depicted in Figure 2.

The structure was found to be dimeric and symmetrical and features both $N(SiMe_3)_2$ substituents as well as both phosphines in a *syn* arrangement. Compared to the cationic stannyl-substituted ylide **IV** reported by Grützmacher and Pritzkow [24], in which the phosphine substituents are in *anti* arrangement, longer Sn1—C1 and shorter P1—C1 bond lengths are observed for **1** (see Table 1 and the Supporting Information, Section S4 re. the calculated *syn*/*anti* energy difference). Both indicate a stronger electron donation from the ylide to the tin atoms in case of **1**. This can be explained by the competition of the ylidyl substituents and the amido ligands in case of **1** and by the higher Lewis acidity of Sn(IV) compared to Sn(II). Compared to the amino(cyanoylidyl)stannylene **III**, the Sn1—C1 bond is slightly shorter, whereas the P1—C1 bond is elongated. This further indicates a stronger electron donation from the ylide to the tin atom, which can be explained by the absence of an anion-stabilizing group (i.e., cyano group in **III**).

NMR analysis indicates that the dimeric structure is retained in solution. In the ^{119}Sn NMR spectrum, a triplet with a chemical shift of $\delta_{119Sn} = 57$ ppm is found. The ^{31}P NMR spectrum shows one singlet at $\delta_{31P} = 28.5$ ppm with pronounced satellites from coupling to the tin nuclei (see Supporting Information). The coupling in the ^{1}H NMR spectrum of the signal from the ylidic hydrogen atom shows a splitting to a multiplet, resting in the coupling to the opposite ylidic hydrogen atom and to both phosphorus atoms, which are magnetically inequivalent (Figure 3).

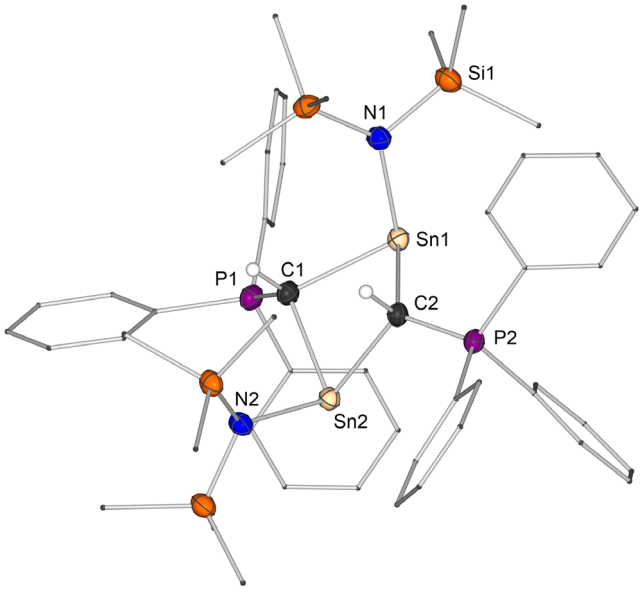

FIGURE 2 | Molecular structure of **1** in the solid-state (ellipsoids at 30% probability). For clarity, hydrogen atoms besides the ylidic are omitted and the phenyl and methyl groups are shown as wireframes. Selected bond lengths (Å) and angles (°): P1—C1 1.713(2), Sn1—C1 2.2885(14), Sn1—C2 2.3056(13), Sn1—N1 2.1589(12), N1—Si1 1.7334(13); P1—C1—Sn1 117.70(7), C1—Sn1—C2 78.75(5), C1—Sn1—N1 106.08(5), and Sn1—N1—Si1 108.57(6).

TABLE 1 | Selected structural parameters of **1**, the isostructural stannylium ion **IV** [24], and the amino(cyano)ylidylstannylene **III** [23].

Structural parameter	1	IV [24]	III [23]
d(Sn1···Sn2)/Å	3.3172(2)	3.320(1)	
d(Sn1—C1)/Å	2.2885(14)	2.245(5)	2.292(2)
d(P1—C1)/Å	1.713(2)	1.759(7)	1.698(2)
∠(C1—Sn1—C2)/°	78.75(5)	84.8(2)	
∠(Sn1—C1—Sn2)/°	92.13(5)	95.3(2)	
∠(P1—C1—Sn1)/°	117.70(7)	125.8(3)	

An AA'XX' spin system can be observed, combined with pronounced satellites from the coupling to ^{117}Sn and ^{119}Sn. Unfortunately, a proper simulation of the experimental spectrum was not possible due to both the broad signals and the tin satellites, which might cover parts of the AA'XX' spin system (see Supporting Information).

2.2 | Coordination Ability

Electron-rich tetrylenes may be used as ligands in transition metal complexes and have been applied for bond activation and catalysis [27].

To estimate the ligand properties, and particularly the donor strength of the stannylene, we treated **1** with gallium chloride in benzene-d_6, since the pyramidalization at the gallium center correlates with the ligands donor capability [28]. The NMR tube was shaken for one minute and after resting for some minutes, colorless crystals were obtained. X-ray structure analysis revealed the formation of the chloro(ylidyl)stannylene $[Ph_3PCH\{SnCl\}]_2$ (**2**) (space group C2/c). The molecular structure is depicted in Figure 4.

Compound **2** is isostructural to **1**, featuring similar bond lengths, and retains the *syn* arrangement of the phosphine substituents and the chlorides. Alternatively, the chloro (ylidyl)stannylene **2** can be obtained from the reaction of $\{(Me_3Si)_2N\}SnCl$ with Ph_3PCH_2 in toluene in 64% isolated yield (Scheme 2).

Product **2** can be isolated by filtration and was washed with hexane. Unfortunately, no NMR analysis was possible due to the poor solubility of **2** in organic solvents. We nevertheless tried to analyze the reaction mixture in more detail.

From the reaction with gallium chloride, an NMR spectrum was recorded immediately after the addition of gallium chloride. In the ^{1}H and ^{31}P NMR spectra, a second species with similar characteristics to **1** can be seen (see Supporting Information). After crystallization of **2**, however, the crystalline material did not dissolve in organic solvents. The observed ^{31}P NMR signal is shifted to higher frequencies ($\delta_{31P} = 29.3$ ppm) compared to **1**. The signal of the ylidic hydrogen atom again shows a characteristic AA'XX' multiplet ($\delta_{1H} = 2.67$ ppm) comparable to **1**.

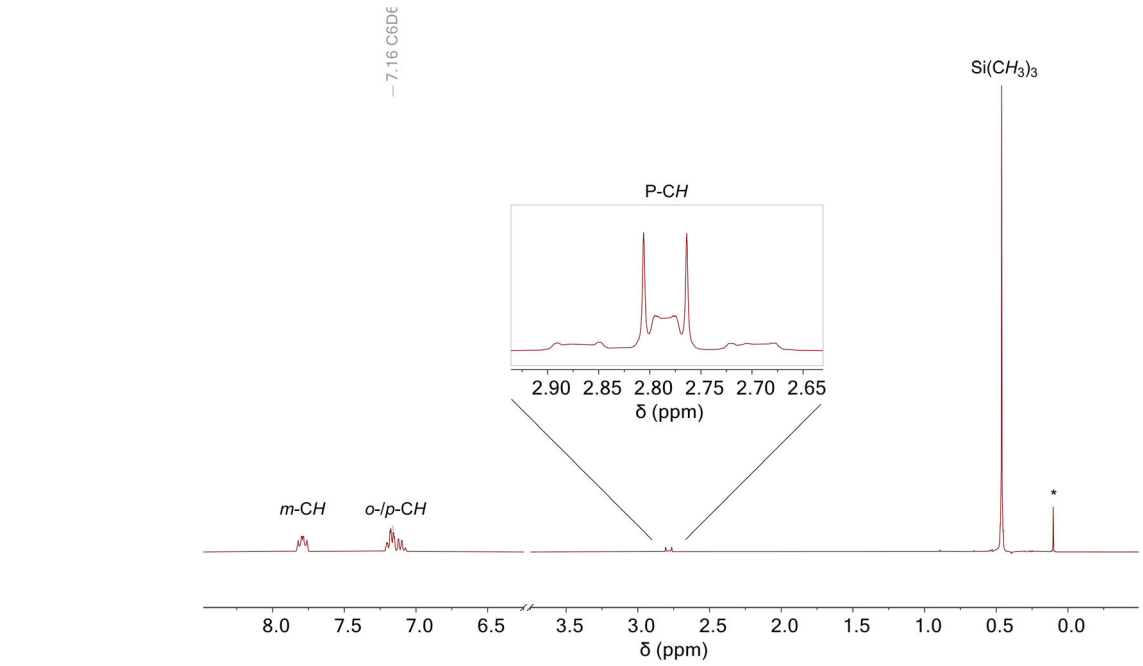

FIGURE 3 | ^{1}H NMR spectrum of **1** in benzene-d_6. The signal of the ylidic hydrogen atom is highlighted. *$HN(SiMe_3)_2$.

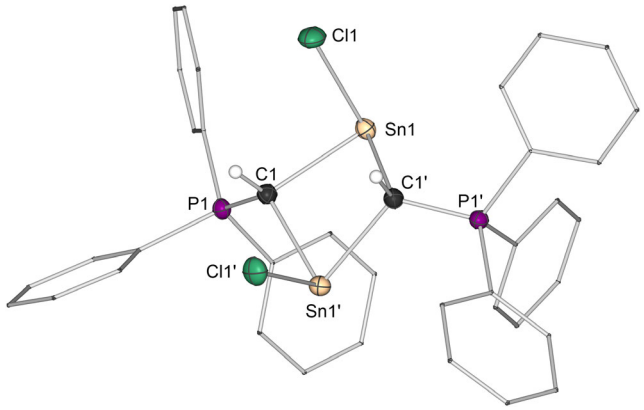

FIGURE 4 | Molecular structure of **2** in the solid-state (ellipsoids at 30% probability). For clarity, hydrogen atoms besides the ylidic are omitted and the phenyl groups are shown as wireframes. Selected bond lengths (Å) and angles (°): P1—C1 1.716(3), Sn1—C1 2.294(3), Sn1—C1' 2.283(3), Sn1—Cl1 2.5217(9), Sn1…Sn1' 3.3735(4); P1—C1—Sn1 117.26(15), C1—Sn1—C1' 79.58(11), C1—Sn1—Cl1 90.28(8), Sn1—C1—Sn1' 94.97(10).

Related compounds are known from the literature. The respective chlorogermylene was synthesized in 2025 by Coburger and coworkers via germyliumylidene transfer [29], and a dimeric chlorogermylene supported by anionic *N*-heterocyclic olefins was published by Rivard and coworkers in 2019 [30].

2.3 | Thermal Stability

From the *syn* arrangement of the amides in **1**, coinciding with the neighboring CH groups, we were interested in the thermal stability and potential *syn* elimination of the amine. Such an elimination would lead to the formation of a conceivable stannaethene of the general formula $[Ph_3PC=Sn]$ or its dimeric or oligomeric ring and cage structures. Potentially, such compounds would form heterocubanes, which are known to form in reactions of amido stannylenes with amines or water [31, 32]. Veith and coworkers obtained Sn_4X_4 heterocubanes (X = NR, O) when the amido-substituted stannylene **VI** was treated with amines or water (Scheme 3).

Power and coworkers investigated the reaction of the diamido tetrylenes $E(N\{SiMe_3\}_2)_2$ (E = Ge, Sn, Pb) toward primary amines. These reactions yielded, for instance, a cyclic trimer $[Ge(NDipp)]_3$ for germanium (Dipp = C_6H_3–2,6-iPr$_2$), whereas the reaction with tin and lead amides led to the formation of

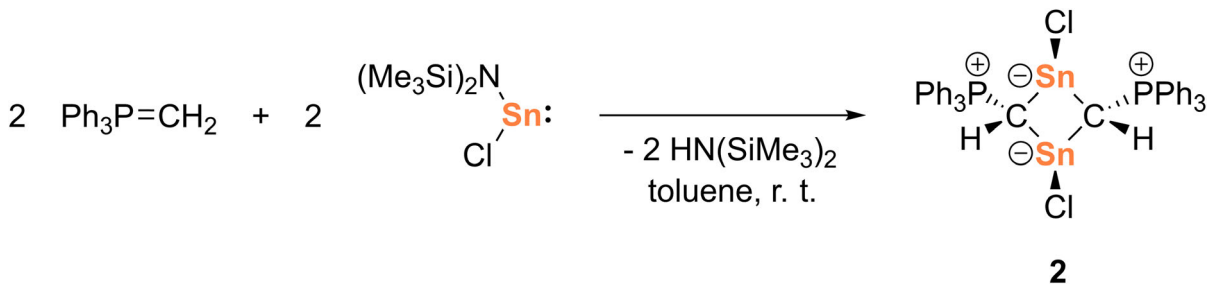

SCHEME 2 | Synthesis of **2**.

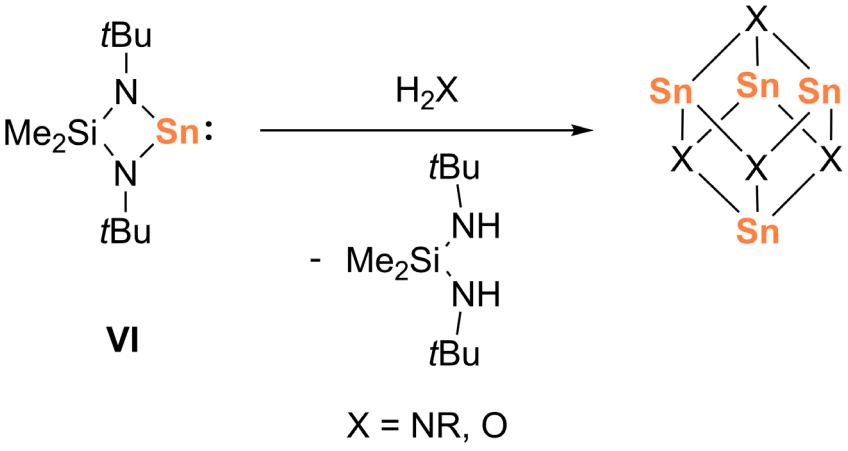

SCHEME 3 | Formation of heterocubanes from the amidostannylene **VI** via deprotonation.

heterocubanes [33]. Wright and coworkers obtained corner-linked double cubanes of the general formula Sn_7N_8 by transamination of primary amines with tin amides [34, 35].

Besides primary amines, our group showed that pyrazoles can also be used as precursors for the synthesis of germanium and tin cages via transamination with the divalent bis(trimethylsilyl)amides [36–38].

When a solution of **1** is heated to 120 °C for 5 h in vacuo, a color change from yellow to red is observed. From a concentrated solution in toluene, we obtained a crop of orange and red crystals. The orange crystals turned out to be the elimination product of two equivalents of the protonated amide. The formation of $HN(SiMe_3)_2$ was confirmed by NMR analysis of the distillate (see Supporting Information). The protons at the ylidic carbon atoms remain, whereas one phenyl group of each phosphine is deprotonated in *ortho* position. Again, a four-membered Sn_2C_2 heterocycle is formed. This time, the tin atoms are connected to the *ortho* position of the triphenylphosphine backbone. Veith and co-workers obtained the same reaction product when the ylide-stabilized amino stannylene is heated to 120 °C in toluene (Scheme 4). The formation of Sn_4C_4 heterocubanes, similar to the reaction with primary amines, was not observed [26]. To best of our knowledge, no Sn_4C_4 heterocubanes are known from the literature.

Compared to **1** and **2**, structural differences can be found in the tin–carbon and phosphorus–carbon bond lengths. For **V**, the Sn—C1 bond length is 1.710(5) Å, compared to 1.7170(13) Å in **1** and 1.716(3) Å in **2**. The P1—C1 bond length in **V** is longer (1.759(7) Å), compared to **1** (1.7170(13) Å) and **2** (1.716(3) Å). The lone pairs at the tin atoms are no longer in *syn* arrangement and are facing opposite directions. Further electronic differences will be discussed in the next paragraph.

The red crystals were also suitable for SC-XRD. Unfortunately, the structure could not be fully refined. From the model, we assume the formation and co-crystallization of the symmetrical Sn_4C_4 heterocubane (about 10%), combined with a disordered structure, in which one tin atom bridges between two ylidic carbon atoms (10%) and an open heterocubane-type Sn_3C_4 cage (80%, **3**; Scheme 5). Assuming that the ylidic entities at the open sites of the cage in **3** are protonated, a cationic entity results; however, although we have made strong attempts in measuring several single crystals from different batches and refining the

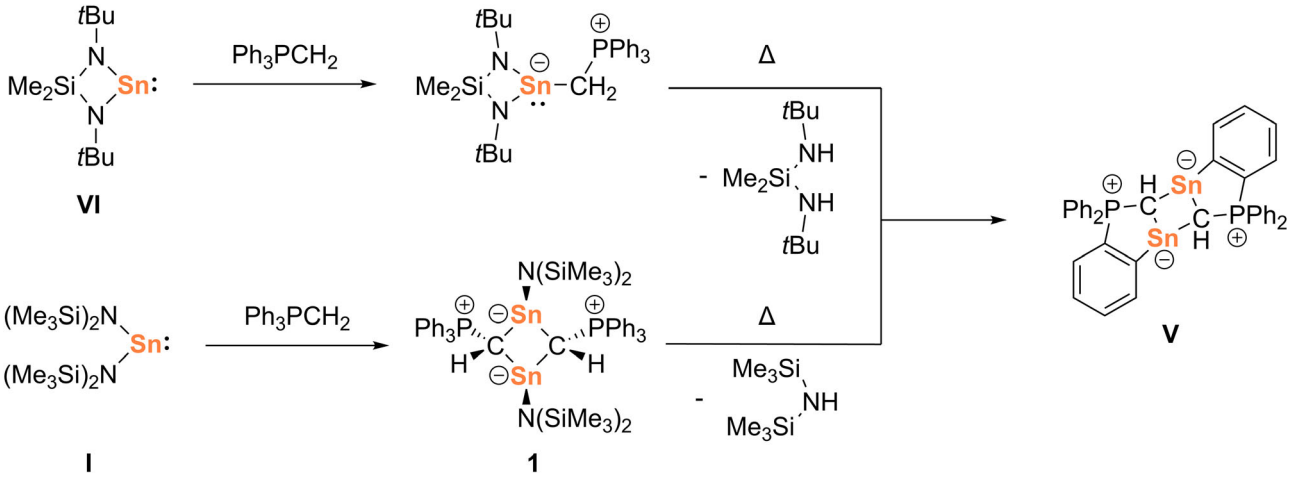

SCHEME 4 | Thermolysis of **1** (bottom) and of a stannylene-ylide adduct, reported by Veith and coworkers (top) [26]. Both reactions lead to the formation of the *ortho*-substituted ylide **V**.

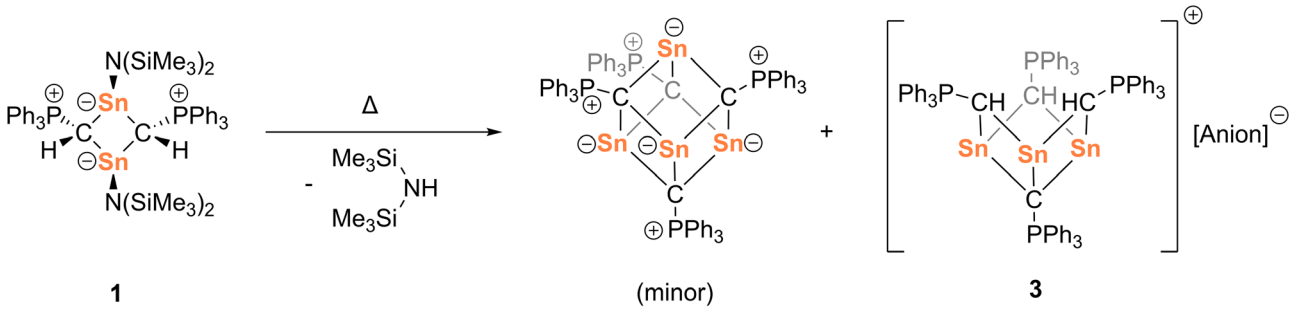

1 (minor) 3

SCHEME 5 | Formation of the Sn_4C_4 heterocubane and the open heterocubane-type Sn_3C_4 cage as product of thermolysis of **1**.

anionic part of **3**, we were not successful. The exact composition remains unresolved since we failed to develop a suitable model due to the geometric arrangement of the residual electron density (see Supporting Information).

NMR analysis of the red crystalline compound failed due to the insolubility of the crystalline material in benzene or THF and decomposition in CD_2Cl_2.

Overall, the thermolysis shows that amino(ylidyl)stannylenes might serve as suitable precursors for the synthesis of Sn_4C_4 heterocubanes. By modification of both, the ylidyl and the amido ligand the synthesis might be optimized in future works.

2.4 | Quantum Chemical Analysis

Density functional theory (DFT) (PBE0/def2-TZVPP//BP86/def2-SVP) studies were performed to analyze the tin–carbon interactions and the potential monomer/dimer equilibrium. No symmetry constraints were applied; therefore, mean values for charges and bond indices are presented. For comparison, the product of thermolysis **V** was included in this description.

For all investigated stannylenes, the dimerization of the hypothetical monomeric form is exergonic. The least differences are obtained for **1**. The change in the free enthalpy amounts to $\Delta G = -13.5$ kcal/mol. For **2**, the dimeric form is about 34.4 kcal/mol more stable. This difference can be explained by the ability of the amido ligand for π-donation to the tin atom and thus stabilizing the monomeric form. For the *ortho*-ylidyl stannylene **V**, the dimerization is highly exergonic ($\Delta G = -468$ kcal/mol).

In case of all stannylenes **1**, **2** and **V**, both highest occupied molecular orbitals are located at the tin atoms, representing the lone pairs (Figure 5). In comparison, the HOMO energy is the lowest for **2**, and the highest is found for **V** (Table 2), indicating enhancing nucleophilicity from **2**, over **1** to **V**. For the HOMO−1 the energy is lower for **V**, compared to **1**.

To analyze the bonding in **1**, **2,** and **V**, we calculated the Wiberg Bond Indices (WBI) and performed Natural Bond Orbital analyses (NBO; Table 3). Additional values are recorded in the Supporting Information.

For the tin–carbon bonds, higher WBIs are obtained for the chlorostannylene **2** compared to **1**. **V** features even higher median WBI. For the ylidic P—C bond, the WBI ascends from **1**, over **V** to **2**. In sum, for all stannylenes **1**, **2,** and **V**, higher WBIs are obtained for the carbon–tin bonds compared to the ylidyl stannylene **III** reported by Gessner and coworkers [23].

NBO analysis shows that the median charge of the tin atoms in **1**, **2,** and **V** is lower compared to stannylene **III**. Therefore, higher covalency of the Sn—C and Sn—N bonds can be assigned in **1**, **2,** and **V**.

The differences between **V** and the stannylenes **1** and **2** arise from the weaker π-donating character of the phenyl moiety compared to the amide in **1**, less pronounced in **2**. This is also displayed in

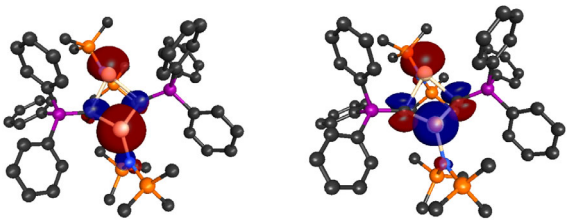

FIGURE 5 | Illustration of both highest occupied MOs of **1** (PBE0/def2TZVPP//BP86/def2-SVP, isovalue: 0.05).

TABLE 2 | HOMO and HOMO−1 energy of **1**, **2**, and **V**.

Frontier orbital energy (eV)	1	2	V
HOMO	−4.702	−5.072	−4.384
HOMO-1	−5.162	−5.902	−5.513

TABLE 3 | WBI for selected bonds and atomic charges *q* according to NBO in **1**, **2**, **V**, and **III** [23].

WBI and NBO charges	1	2	V	III [23]
Sn1—C1	0.61	0.65	0.64	0.44
Sn1—C2	0.60	0.62	0.65	
P1—C1	1.14	1.27	1.20	1.09
q(Sn)	1.23	0.98	0.86	1.29
q(C1)	−1.67	−1.53	−1.43	−1.19
q(P)	1.65	1.62	1.60	1.65

the WBI of the C1—Sn1 bonds. In the *ortho*-substituted stannylene **V**, higher WBIs are obtained. The NBO charges for the tin atoms are decreased, whereas the ylidic carbon atoms bear an increased charge. This further indicates a stronger electron donation from the ylide to the tin atom and a more effective stabilization through the ylide, leading to a more electron-rich stannylene.

Additionally, Quantum Theory of Atoms in Molecules (QTAIM) analysis was performed for **1**. For comparison, the tin–carbon, tin–nitrogen, and phosphorus–carbon bonds are evaluated. The mean value for the electron density at the bond-critical points between the Sn—C bonds is 0.074, indicating an ionic character, in the range of typical metal-ligand contact. The positive Laplacians ($\Delta = 0.1$) suggest closed-shell interactions. Overall, a stabilizing ionic bond with covalent bonding components, indicated by the negative enthalpy, can be seen. By the low value for the ellipticity, no π-contribution to the carbon–tin bond is observable. Compared to the tin–carbon bonds, higher densities are obtained at the bond critical points (BCPs). The ylidic P—C bonds, on the other hand, are covalent, and by the ellipticity, partial π-bonding is observable. This suggests that the electron donation from the ylide to the tin centers is incomplete and hindered due to the dimerization and the competition with the amide.

3 | Conclusions

In summary, we presented the synthesis of ylidylstannylenes starting from readily available tin bis(trimethylsilyl)amides and one of the simplest Wittig ylides via deprotonation. The amido(ylidyl)stannylene **1** and the chloro(ylidyl)stannylene **2** feature dimeric structures, forming a four-membered Sn_2C_2 cycle in solid state and in solution. **1** can be further used for the synthesis of an *ortho*-ylidyl substituted stannylene via thermal amide elimination. Additionally, we obtained crystals from one product of the thermolysis which indicates that the dimeric amino(ylidyl) stannylene and related compounds might serve as precursors for Sn_4C_4 heterocubanes. Due to the simple synthesis of the stannylene, backbone modification of the ylide or replacing the amine for another might enable the cubane synthesis. Inspired by these findings, the investigation of other electron-rich amino(ylidyl)tetrylenes is part of current research in our laboratories.

4 | Experimental Section

4.1 | General Methods

All operations were carried out under dry argon using standard Schlenk and glovebox techniques. $Sn(N\{SiMe_3\}_2)_2$ [19], $Sn(N\{SiMe_3\}_2)Cl$ [39] and Ph_3PCH_2 [40] were prepared according to literature procedures. Solvents were dried over Na/K or CaH_2 and rigorously degassed before use. NMR spectra were recorded on a Bruker Avance Neo 400 or an Avance 300 spectrometer operating at ^1H Larmor frequencies of 400 or 300 MHz in dry degassed deuterated solvents. ^1H, $^{13}C\{^1H\}$, and $^{29}Si\{^1H\}$ chemical shifts were reported against TMS, $^{31}P\{^1H\}$ against H_3PO_4 and $^{119}Sn\{^1H\}$ against $SnMe_4$. Coupling constants (J) are given in Hertz as positive values, regardless of their real individual signs. The multiplicity of the signals is indicated as s, d, q, sept, or m for singlet, doublet, quartet, septet, or multiplet, respectively. The assignments were confirmed, as necessary, with the use of 2D NMR correlation experiments. The MestreNova software package was used for analyzing the spectra. IR spectra were measured on a Bruker Alpha spectrometer using the attenuated reflection technique (ATR), and the data are quoted in wavenumbers (cm^{-1}). The intensity of the absorption band is indicated as vw (very weak), w (weak), m (medium), s (strong), vs (very strong), and br (broad). Elemental analyses were carried out in the institutional technical laboratories of the Karlsruhe Institute of Technology (KIT). Elemental analysis data were gathered from isolated crystalline material of the corresponding compound and reported as obtained, even if the established deviation of ±0.4% was not reached, as these requirements were shown to be misleading in some cases [41].

Diffraction data were measured using a Stoe IPDS II diffractometer and graphite-monochromated MoK_α (0.71073 Å) radiation. Absorption corrections were carried out using the STOE LANA [42] software package by scaling of diffraction intensities. The structures were solved in OLEX2 1.5 [43] by dual-space direct methods with SHELXT [44], followed by full-matrix least-squares refinement using SHELXL-2014/7 [45]. All non-hydrogen atoms were refined anisotropically. The contribution of the hydrogen atoms, in their calculated positions, was included in the refinement using a riding model. A full listing of atomic coordinates, bond lengths, angles, and displacement parameters has been deposited at the Cambridge Crystallographic Data Centre with deposition numbers 2 547 696 and 2 547 697 for **1** and **2**, respectively.

4.2 | Preparation of 1

A Schlenk tube was charged with $Sn(N\{SiMe_3\}_2)_2$ (318 mg, 0.724 mmol, 1.00 equiv.) and Ph_3PCH_2 (200 mg, 0.724 mmol, 1.00 equiv.). To this mixture, toluene (5 ml) was added. The resulting orange solution was stirred for 16 h. Afterwards, the solvent was removed in vacuo. The residue was extracted with hexane (10 ml), and the yellow solution was concentrated to incipient crystallization. Overnight, yellow crystals formed, which were isolated and dried in vacuo. **1** was obtained as yellow, crystalline solid (233 mg, 0.210 mmol, 58%).

^1H NMR (300 MHz, C_6D_6): δ (ppm) = 7.79 (m, 12H, *m*-CH), 7.22–7.06 (m, 18H, *o*- und *p*-CH), 2.90–2.67 (m, 2H, C^1H), 0.46 (s, 36H, CH_3).

$^{13}C\{^1H\}$ NMR (101 MHz, C_6D_6): δ (ppm) = 133.95 (*pseudo*-t, J = 4.8 Hz, *m*-*C*H), 131.75 (s, *p*-CH), 131.44 (m, *i*-*C*), 130.54 (m, *i*-*C*), 128.99–128.72 (m, *o*-*C*H), 14.08 (m, C^1), 8.00 (s, CH_3).

$^{29}Si\{^1H\}$ NMR (79 MHz, C_6D_6): δ (ppm) = −0.99 (s).

$^{31}P\{^1H\}$ NMR (122 MHz, C_6D_6): δ (ppm) = 28.52 (s).

$^{119}Sn\{^1H\}$ NMR (149 MHz, C_6D_6): δ (ppm) = 57.02 (t, $^2J_{Sn\text{-}P}$ = 133.5 Hz).

IR (ATR): $\tilde{\nu}$ (cm^{-1}) = 3053 (vw), 2945 (w), 2888 (vw), 1483 (vw), 1435 (m), 1237 (m), 1187 (vw), 1101 (m), 997 (vw), 976 (vw), 934 (s), 839 (vs), 772 (m), 742 (s), 712 (s), 690 (vs), 658 (s), 606 (m), 534 (vs), 503 (s), 482 (w), 474 (w), 464 (w), 455 (w), 428 (w), 415 (vw), 404 (vw).

Elemental analysis (calc., found for $C_{50}H_{68}N_2P_2Si_4Sn_2$): C (54.2, 54.4), H (6.18, 5.98), N (2.52, 1.70).

4.3 | Reaction of 1 With $GaCl_3$

1 (10 mg, 9 μmol, 1.00 equiv.) was placed in a Young capped NMR tube and dissolved in C_6D_6 (0.4 ml). Gallium chloride (3 mg, 18 μmol, 2.00 equiv.) was added. The NMR tube was shaken for 1 minute and left to rest. NMR spectra were recorded (see Supporting Information).

4.4 | Preparation of 2

A Schlenk tube was charged with $Sn(N\{SiMe_3\}_2)Cl$ (71 mg, 0.26 mmol, 1.00 equiv.) and Ph_3PCH_2 (81 mg, 0.26 mmol, 1.00 equiv.). To this mixture, toluene (3 ml) was added. The reaction mixture turned cloudy, and a precipitate was formed. The reaction mixture was then stirred for 16 h. Afterwards, the supernatant solution was decanted. The residue was washed with hexane (3 ml) and dried in vacuo. The product was obtained as a pale-yellow solid (71 mg, 0.08 mmol, 64%).

The ^1H and ^{31}P NMR data are obtained from the NMR of the reaction mixture of **1** with $GaCl_3$ and not from the pure compound. Due to the poor solubility of **2**, no ^{13}C or ^{119}Sn NMR analysis was possible.

^1H NMR (400 MHz, C_6D_6) δ = 7.73–7.65 (m, 12H, *m*-CH), 7.25–7.19 (m, 12H, *o*-CH), 7.13–7.06 (m, 6H, overlapping with *p*-CH), 2.73–2.57 (m, 1H, C^1H).

$^{31}P\{^1H\}$ NMR (162 MHz, C_6D_6): δ (ppm) = 29.25 (s).

IR (ATR): $\tilde{\nu}$ (cm^{-1}) = 3051 (vw), 2982 (vw), 1588 (vw), 1483 (vw), 1437 (m), 1332 (vw), 1312 (vw), 1115 (w), 1100 (m), 995 (vw), 973 (m), 861 (s), 820 (w), 745 (m), 714 (s), 691 (vs), 551 (s), 534 (vs), 526 (vs), 505 (s), 467 (w), 429 (vw).

Elemental analysis (calc., found for $C_{38}H_{32}Cl_2P_2Sn_2$): C (53.14, 53.42), H (3.76, 4.07).

4.5 | Thermolysis of 1

A Schlenk tube was charged with **1** (40.0 mg, 36.1 μmol) and connected to a second Schlenk tube with a knee. The apparatus was evacuated (10^{-3} mbar). The empty Schlenk tube was cooled with liquid nitrogen, and the other Schlenk tube was heated to 140°C for 4 h with an oil bath. The initially yellow solid changed its color to red. Afterwards, the Schlenk tubes were disconnected, and NMR spectra were recorded (see Supporting Information). Toluene (2 ml) was added to the red solid. **V** precipitated from the red solution and was isolated (3 mg, 3.8 μmol, 11%). The toluene solution was decanted and concentrated under reduced pressure. After one week, a small number of red crystals of **3** formed.

Acknowledgments

The authors acknowledge support by the German Research Foundation (DFG) through grant no BR 2169/5-1 (535548579). Support by the state of Baden-Württemberg through bwHPC and the German Research Foundation (DFG) through grant no INST 40/575-1 FUGG (JUSTUS 2 cluster) is also acknowledged. This work was financially supported by the Fonds der Chemischen Industrie through a Kekulé scholarship for P. W. We thank A. H. for help with NMR analysis and S. W. for help with SC-XRD. Furthermore, the authors thank H. B. and A. R. for NMR spectroscopic measurements and N. K. for elemental analysis.

Open Access funding enabled and organized by Projekt DEAL.

Funding

Deutsche Forschungsgemeinschaft (BR 2169/5-1 (535548579), INST 40/575-1 FUGG (JUSTUS 2 cluster)); Fonds der Chemischen Industrie.

Conflicts of Interest

The authors declare no conflicts of interest.

Data Availability Statement

The data that support the findings of this study are available in the supplementary material of this article.

References

1. M. Veith, O. Recktenwald, "Organotin Compounds," in Topics in Current Chemistry, vol. 104 (1982): 1–55.

2. V. I. Shiryaev and V. F. Mironov, "Bivalent Tin Analogues of Carbenes," *Russian Chemical Reviews* 52 (1983): 184–200.

3. B. Gehrhus, P. B. Hitchcock, M. F. Lappert, J. Heinicke, R. Boese, and D. Bläser, "Synthesis, Structures and Oxidative Addition Reactions of New Thermally Stable Silylenes; Crystal Structures of [(CH2tBu)}2C6H4-1,2] and [((CH2tBu)}2C6H4-1,2)(μ-E)]2 (E = Se or Te)," *Journal of Organometallic Chemistry* 521 (1996): 211–220.

4. B. Gehrhus and M. F. Lappert, "Reactions of the Stable Bis(amino)silylene with Multiply Bonded Compounds," *Polyhedron* 17 (1998): 999–1000.

5. M. Haaf, T. A. Schmedake, and R. West, "Stable Silylenes," *Accounts of Chemical Research* 33 (2000): 704–714.

6. S. Nagendran and H. W. Roesky, "The Chemistry of Aluminum(I), Silicon(II), and Germanium(II)," *Organometallics* 27 (2008): 457–492.

7. Y. Mizuhata, T. Sasamori, and N. Tokitoh, "Stable Heavier Carbene Analogues," *Chemical Reviews* 109 (2009): 3479–3511.

8. M. Asay, C. Jones, and M. Driess, "*N*-Heterocyclic Carbene Analogues with Low-Valent Group 13 and Group 14 Elements: Syntheses, Structures, and Reactivities of a New Generation of Multitalented Ligands," *Chemical Reviews* 111 (2011): 354–396.

9. A. V. Zabula and F. E. Hahn, "Mono- and Bidentate Benzannulated N-Heterocyclic Germylenes, Stannylenes and Plumbylenes," *European Journal of Inorganic Chemistry* 2008 (2008): 5165–5179.

10. Y. Peng, B. D. Ellis, X. Wang, and P. P. Power, "Diarylstannylene Activation of Hydrogen or Ammonia with Arene Elimination," *Journal of the American Chemical Society* 130 (2008): 12268–12269.

11. Y. Peng, M. Brynda, B. D. Ellis, J. C. Fettinger, E. Rivard, and P. P. Power, "Addition of H2 to Distannynes Under Ambient Conditions," *Chemical Communications* (2008): 6042–6044.

12. T. J. Hadlington and C. Jones, "A Singly Bonded Amido-Distannyne: H2 Activation and Isocyanide Coordination," *Chemical Communications* 50 (2014): 2321–2323.

13. S. Freitag, K. M. Krebs, J. Henning, J. Hirdler, H. Schubert, and L. Wesemann, "Stannylene-Based Lewis Pairs," *Organometallics* 32 (2013): 6785–6791.

14. K. Oberdorf and C. Lichtenberg, "Small Molecule Activation by Well-Defined Compounds of Heavy p-Block Elements," *Chemical Communications* 59 (2023): 8043–8058.

15. M. P. Coles, "The Role of the Bis-Trimethylsilylamido Ligand, [N{SiMe3}2]−, in Main Group Chemistry. Part 1: Structural Chemistry of the s-Block Elements," *Coordination Chemistry Reviews* 297–298 (2015): 2–23.

16. M. P. Coles, "The Role of the Bis-Trimethylsilylamido Ligand, [N{SiMe3}2]−, in Main Group Chemistry. Part 2: Structural Chemistry of the Metallic p-Block Elements," *Coordination Chemistry Reviews* 297–298 (2015): 24–39.

17. A. Sarbajna, V. Swamy, and V. H. Gessner, "Phosphorus-Ylides: Powerful Substituents for the Stabilization of Reactive Main Group Compounds," *Chemical Science* 12 (2020): 2016–2024.

18. A. Das, Q. Le Dé, and V. H. Gessner, "Rethinking Carbanion Chemistry from Donor Substituents to Weakly Coordinating Carbanions," *Nature Reviews Chemistry* 9 (2025): 1–14.

19. D. H. Harris and M. F. Lappert, "Monomeric, Volatile Bivalent Amides of Group IV_B Elements, $M(NR^1{}_2)_2$ and $M(NR^1R^2)_2$ (M=Ge, Sn, or Pb; R^1=Me_3 Si, R^2=Me_3C)," *Journal of the Chemical Society, Chemical Communications* (1974): 895–896.

20. R. Akhtar, K. Gaurav, and S. Khan, "Applications of Low-Valent Compounds with Heavy Group-14 Elements," *Chemical Society Reviews* 53 (2024): 6150–6243.

21. A. Schmidpeter, H. P. Schrodel, and J. Knizek, "2-Stannaindenes and 2-Stannaindanes," *Heteroatom Chemistry* 9 (1998): 103–108.

22. C. Mohapatra, L. T. Scharf, T. Scherpf, et al., "Isolation of a Diylide-Stabilized Stannylene and Germylene: Enhanced Donor Strength through Coplanar Lone Pair Alignment," *Angewandte Chemie International Edition* 58 (2019): 7459–7463.

23. V. S. V. S. N. Swamy, M. Kumar, F. Krischer, K. S. Feichtner, B. Mallick, and V. H. Gessner, "Synthesis and Reactivity of Amino(Ylide)Stannylenes," *Zeitschrift Für Anorganische Und Allgemeine Chemie* 650 (2024): e202400079.

24. H. Grutzmacher and H. Pritzkow, "Reaction of Stannyl-Substituted Phosphorus Ylides with Boron Trifluoride Diethyl Etherate: Evidence for Formation of Transient Triphenylphosphonio-Substituted Stannaethenes," *Organometallics* 10 (1991): 938–946.

25. F. Krämer, M. Radius, A. Hinz, M. E. A. Dilanas, and F. Breher, "Accessing Cationic α-Silylated and α-Germylated Phosphorus Ylides," *Chemistry – A European Journal* 28 (2022): e202103974.

26. M. Veith and V. Huch, "Cyclische Diazastannylene," *Journal of Organometallic Chemistry* 308 (1986): 263–279.

27. T. J. Hadlington, "Heavier Tetrylene- and Tetrylyne-Transition Metal Chemistry: It's No Carbon Copy," *Chemical Society Reviews* 53 (2024): 9738–9831.

28. A. El-Hellani, J. Monot, S. Tang, R. Guillot, C. Bour, and V. Gandon, "Relationship between Gallium Pyramidalization in L·$GaCl_3$ Complexes and the Electronic Ligand Properties," *Inorganic Chemistry* 52 (2013): 11493–11502.

29. D. Zuber, S. Frei, and P. Coburger, "π-Complexes of Main-Group Metal Cations: Exploration of Lewis Acid Reactivity," *ChemistryEurope* 3 (2025): e202500199.

30. E. Hupf, F. Kaiser, P. A. Lummis, et al., "Linking Low-Coordinate Ge(II) Centers via Bridging Anionic N-Heterocyclic Olefin Ligands," *Inorganic Chemistry* 59 (2020): 1592–1601.

31. M. Veith, "Unsaturated Molecules Containing Main Group Metals," *Angewandte Chemie International Edition in English* 26 (1987): 1–14.

32. M. Veith and G. Schlemmer, "Cyclische Diazastannylene, XIII. $[SnN_2(CH_3)_2]_4$ Und $[SnNCH(CH_3)_2]_4$, Moleküle Mit Cuban-Struktur," *Chemische Berichte* 115 (1982): 2141–2152.

33. H. Chen, R. A. Bartlett, H. V. R. Dias, M. M. Olmstead, and P. P. Power, "Synthesis and Structural and Spectroscopic Characterization of the Germanazene [GeN(2,6-i-Pr2C6H3)]3 and the Tin and Lead Tetramers [SnN(BMes2)]4, [SnN(2,6-i-Pr2C6H3)]4, and [PbN(2,6-i-Pr2C6H3)]4," *Inorganic Chemistry* 30 (1991): 3390–3394.

34. D. R. Armstrong, F. Benevelli, A. D. Bond, et al., "Formation of Double Cubanes $[Sn_7(NR)_8]$ in the Reactions of Pyridyl and Pyrimidinyl Amines with $Sn(NMe_2)_2$: A Synthetic and Theoretical Study," *Inorganic Chemistry* 41 (2002): 1492–1501.

35. F. Benevelli, E. L. Doyle, E. A. Harron, et al., "Ligand-Directed Structural Modification of Imidotin(II) Cubanes: The Mixed Oxidation State Double-Cubanes [Sn7{2-NR}8]·n THF (R=Pyrimidinyl, 5-Methylpyridinyl)," *Angewandte Chemie International Edition* 112 (2000): 1501–1503.

36. I. Krummenacher, C. Oschwald, H. Rüegger, and F. Breher, "Cationic Main Group Element Cages of Germanium(II) and Tin(II) Consisting of 3,5-Di(*t* -butyl) Substituted Pyrazolyl Ligands in the Bridging Position," *Zeitschrift Fur Anorganische Und Allgemeine Chemie* 633 (2007): 2354–2361.

37. F. Breher and H. Rüegger, "Distannenes Turned Inside Out: Bis(stannylenes) with an Unusual Structural Motif," *Angewandte Chemie International Edition* 44 (2005): 473–477.

38. I. Krummenacher, I. Fernández, H. Rüegger, F. Weigend, and F. Breher, "Phosphine-Functionalised Tris(pyrazolyl)methane Ligands and their Mono- and Heterobimetallic Complexes," *Dalton Transactions* 48 (2009): 5335–5347.

39. R. W. Chorley, P. B. Hitchock, B. S. Jolly, M. F. Lappert, and G. A. Lawless, "Crystalline Binuclear Cis- and Trans-Chlorotin(II) Amides $[Sn(\mu\text{-}Cl)(NR_2)]_2$, the Cis-1a⇌trans-1b Isomerisation for [NR_2 = $NCMe_2(CH_2)_3CMe_2$], and the X-Ray Structures of 1a and of Trans-$[Sn(\mu\text{-}Cl)\{N(SiMe_3)_2\}]_2$," *Journal of the Chemical Society. Chemical Communications* (1991): 1302–1303.

40. R. Köster, D. Simić, and M. A. Grassberger, "Zur Darstellung Salzfreier Trialkyl-alkylidenphosphorane," *Justus Liebigs Annalen Der Chemie* 739 (2006): 211–219.

41. R. E. H. Kuveke, L. Barwise, Y. van Ingen, et al., "An International Study Evaluating Elemental Analysis," *ACS Central Science* 8 (2022): 855–863.

42. J. Koziskova, F. Hahn, J. Richter, and J. Kožíšek, "Comparison of Different Absorption Corrections on the Model Structure of Tetrakis(μ_2-Acetato)-Diaqua-Di-Copper(II)," *Acta Chimica Slovaca* 9 (2016): 136–140.

43. O. V. Dolomanov, L. J. Bourhis, R. J. Gildea, J. A. K. Howard, and H. Puschmann, "*OLEX2* : A Complete Structure Solution, Refinement and Analysis Program," *Journal of Applied Crystallography* 42 (2009): 339–341.

44. G. M. Sheldrick, "*SHELXT* – Integrated Space-Group and Crystal-Structure Determination," *Acta Crystallographica. Section A, Foundations and Advances* 71 (2015): 3–8.

45. G. M. Sheldrick, "Crystal Structure Refinement with SHELXL," *Acta Crystallographica. Section C, Structural Chemistry* 71 (2015): 3–8.

Supporting Information

Additional supporting information can be found online in the Supporting Information section.